Design, Modeling and Manufacturing a New Robotic Gripper with High Load Bearing Capability and Robust Control of its Mechanical Arm

Vahid Boomeri
Department of Mechanical Engineering, Faculty of Engineering,
University of Kharazmi, Tehran, Iran
E-mail: vahidviolin@gmail.com

Hami Tourajizadeh*
Department of Mechanical Engineering, Faculty of Engineering,
University of Kharazmi, Tehran, Iran
E-mail: Tourajizadeh@khu.ac.ir ,
*Corresponding author

Received: 26 June 2019, Revised: 2 September 2019, Accepted: 17 September 2019

Abstract: In this paper, a new robotic gripper is proposed and modeled which is able to bear a high amount of load and it can be used as the claws of climbing robots. As the climbing robots are usually heavy and their configuration should be kept in height against the gravity, firm grippers with no slippage possibility should be designed in order to guarantee the stability. The proposed new gripper is essentially required for the grip-based climbing robots which are heavy and are supposed to accomplish a specific operational task while they are grasping the pipe-shaped structures. The kinematic and quasi-static modeling of the proposed gripper is extracted and its related parameters are optimized to provide the maximum gripping force and the minimum slippage probability. Since these robust grippers are usually actuated by high torque motors, the reaction effect of the actuators force on the arm of the robot model is investigated here as a new study. Hence, the corresponding mechanical arm is also controlled, using a robust nonlinear controller to neutralize the destructive effect of extreme reaction forces or torques from the gripper motors to the robot arm during its mission. Thus, a robust controller is designed and implemented on the arm joint to cover the required positioning accuracy of the arm movement during the climbing motion. Afterward, the applicability of the proposed gripper and also the efficiency of the designed controller is verified by the aid of some analytic and comparative simulation scenarios performed in MATLAB-SIMULINK and MSC-ADAMS simulation. It is shown that the proposed gripper together with its related controlling algorithm for the arm can successfully provide a proper climbing mechanism for these kinds of robots which are supposed to climb through the structures and perform a special manipulating task.

Keywords: Climbing Robot, Gripper Mechanism, Optimal Design, Robust Controller, Sliding Mode Control

Reference: Vahid Boomeri, Hami Tourajizadeh, "Design, Modeling and Manufacturing a New Robotic Gripper with High Load Bearing Capability and Robust Control of its Related Mechanical Arm", Int J of Advanced Design and Manufacturing Technology, Vol. 14/No. 1, 2021, pp. 1–17. DOI: 10.30495/admt.2021.1872367.1131

Biographical notes: Vahid Boomeri received his BSc in Mechanical Engineering from the University of Semnan in 2015 and at present he is MSc student of Kharazmi university. One scientific research paper and two conference papers are the results of his researches on parallel robots and robust control. **Hami Tourajizadeh** received his PhD from IUST in the field of mechanics, where more than 50 journals and conference papers are the results of his researches so far. He is now an assistant professor of Kharazmi University since 2013. His research interests include robotics, control, and optimization.

 © 2021 IAU, Majlesi Branch

1 INTRODUCTION

Nowadays, a large number of robotic end-effectors are made which are responsible to perform inspectional or operational tasks like sensing, lasing, citing, welding and even load-carrying operations. In other word, the end-effector is the boundary between the robot and its interacting environment. Hence, the criteria of designing a tool as an autonomous or semi-autonomous system should be discussed according to the tasks, sequences of their operations, workstations, design optimization considerations, type of operations like handling, grasping, pick and place procedures and etc. A vast amount of robots and robotic systems needs a gripper shape mechanism either for their locomotion procedure or implementing their operational tasks. For example, in load-carrying operations, generally, a gripper-based mechanism is demanded to accomplish their corresponding missions. In this paper, a gripper tool is investigated.

According to the required tasks, different kinds of grippers are proposed to accomplish the duties of the robots in order to perform the final operation. So, a proper mechanism should be proposed for a gripper which is supposed to perform a special task. The configuration choice is a frequent apprehension for designers so the proper configuration choice should be investigated precisely for a good systematic robotic cell design. Considering the fact that 15-70% of the total cost of a manufactured system is spent on handling operations, the tooling procedure must be considered through designing a robot based on RC (Robotic Cell) aspects and the gripper should be designed as a handling tool in a robotic cell planning [1]. The investigation of a proper tool for a robotic system is not limited to the mechanism design but also the effect of the gripper on the system base should be considered too. This is contributed to the fact that the operation of a tool in the final step of its operation as an end-effector can affect the base system behavior.

In this paper, the effect of the designed gripper on its related robotic arm is also investigated. There are a lot of criteria parameters for designing the robotic gripper including their dexterity, stiffness, compliance, robustness, applicability and etc. each of them needs special consideration for their styling design, mechanism design, kinematics, kinetics and etc [2]. One of the most famous designs of these kinds of grippers is inspired by human or animal hands. These kinds of grippers have a lot of degrees of freedom and their control procedure is challenging, however, their advantage is their high adaptability and dexterity which can grasp the objects with different shapes. The other cases of grippers have a simpler structure with a lower amount of DOFs motivated by two or more moving fingers which are designed for object handling. Here some of the famous kinds of the grippers are reviewed for each case, different kinds of grippers are designed according to their special applications.

SLUM(Self-Locking Underactuated Mechanism) gripper [3] is a three fingers gripper for which each finger has two DOFs (degrees of freedom) which is driven by only one central actuator so this gripper is an underactuated mechanism and is designed for handling objects with different geometrical shapes with good adaptivity. The SLUM gripper is a complicated gripper which cannot be used easily. Another sample of the underactuated grippers is GR2 [4] which has two fingers with the structure of four-bar parallel mechanisms. The mechanism is controlled using two motors. The grasping task can be performed through two phases called object-covering and locking operations.

LARM is another gripper based on the human hand [5]. This gripper has three fingers and each finger has one degree of freedom and is able to grasp the cylindrical, spherical or cubic objects. In some grippers, all of the joints are active joints(fully-actuated) [6]. These kinds of grippers are able to handle any object with any geometrical shapes with good stability. In some artificial hands [7], cables and pulleys are employed to increase the operation speed and the exerted force for sensitive tasks equipped by a 3D thumb in order to provide forces up to 100 Newtons. Simplicity and low-cost production is a target which should be considered for designing a system. This issue is not considered in hand grippers since lots of DOFs and motors are employed in them which is not suitable for simple mechanism design and is not financially or technically optimum. The material which the grippers are made from is also significant to cover the special applications of the designed grippers. For example, the material of the gripper designed in [8] is made from silicone which can provide good compliance and adaptability to encompass the target objects by the aid of a simple linear actuator.

Some grippers are formed as a single closed-loop structure to hold the objects. These grippers curl around the objects like a camera lens with a controllable contact force. An example of this kind of grippers can be seen in [9] in which a 12-bar parallel mechanism is employed to provide a four DOFs gripper. This gripper can hold the objects and can move them slightly in a planar trajectory. Most of the grippers employ lever-based force to provide big contact forces however, some grippers use wedge-based force to exert big contact force. SGM (Spherical Gripper Mechanism) [10] is an example of this kind of grippers which is a spherical mechanism and is able to hold the objects with different geometrical shapes but within a limited sized. In that research, static analysis is investigated by virtual work method for SGM. The previously mentioned grippers are a tool to hold and handle the objects while a complicated application can be considered for grippers.

© 2021 IAU, Majlesi Branch

As it is the aim of our proposed gripper in this paper, grippers can be designed and implemented for weight supporting purposes. This application is common in robotics and is inspired by animals like apes that use their hands and tails for climbing trees. It should be declared that the ape's hand duty is not limited to simple grasping or object holding like fruits but also its hands can be used as a support member to keep the animal body on trees. The main application of the mentioned grippers is for climbing robots. To meet this goal, a strong gripper is needed which could be able to grasp and hold a bar or a pipe firmly without slippage. The stability of the climbing robot depends on its related grippers since the total weight of the robot is tolerated by the grippers as the support points for the robot. One of the best grippers manufactured to cover the mentioned target is Climbot [11]. This robot gripper has two fingers, each gripper is a four-bar linkage mechanism with a worm-gear transmission system to provide the required normal force.

The same structure is employed in [12] for 3Dclimber with a V-shape mechanism that is able to grasp the pipes with circular shapes cross-section and support the robot movement without slippage. The two-finger mechanism is also used in Raupi [13] by which the contact with bars can be detected by using the installed micro switches and is able to provide up to 46-newton force for supporting a 2-kilogram robot by using the special gearbox. ROMA [14] is another gripper-based climbing robot in which the grippers are controlled by linear motors with mechanical brake to grasp the pipes and climb the metallic infrastructures. The gripper mechanisms are not only based on human fingers. Some of them are designed according to the hook structure which are employed in robots that ascend through the rocks and cliffs [15].

One of the essential studies to design a gripper is modeling the kinematics and statics of the related mechanism which shows the efficiency and applicability of the designed gripper. These studies are performed in the following researches. Rahman et al [16]. have performed the static and control analysis of a modular gripper with four fingers in which three phases of transformation, grasping and releasing are studied. Also Heidari et al. [17] have studied the kinematics and stability of an underactuated two-fingered gripper with the ability to hold and move cylindrical and spherical objects. Kinematics and geometrical analysis of MESO [18] gripper are done in which the designed gripper can grasp tiny and delicate objects like nails with only two fingers. In this paper, a new gripper is designed and proposed which can tolerate heavy loads that the proposed gripper can be treated as a supporting member for climbing robots which move through infrastructures and trusses without the risk of slippage just like the monkey's hands which help them to swing through the branches of trees. The proposed gripper is modeled and its related kinematics and statics are extracted. The geometrical specification of the gripper is then optimized according to the extracted model, for example, the position of the gripper actuator. The efficiency of the designed gripper is verified by modeling the gripper in MATLAB and MSC_ADAMS and the proposed gripper is then manufactured according to this model.

It is shown that the proposed gripper is able to support a 20 kg robot successfully. Not only the gripper can grasp the exact position of the bars accurately but also is able to provide sufficient normal force so the generated friction force can neutralize the destructive effect of backlash torque of climbing operation from climbing robot's main motors and to avoid its probable slippage. In the previous works, the calculations related to robust grasping is missed and the non-slippage condition for grippers is not discussed either. They usually focus on grasping procedure for grippers in order to encompass the objects with different shapes while about the firm grasping with no slippage, no special research is conducted. For example, for UHVAT [19] (Usable Holding Versatile Adjustable Tool) gripper, only the kinematics of the gripper is extracted while its static formulation is ignored. However, in the present work, the grasping robustness is also investigated according to static equations which is not considered for UHVAT. This study is required to ensure that the gripper is able to grasp an object firmly and provide the stability of the robot in height without slipping or releasing possibility during the grasp operation and under the external forces including the gravity and the robot's motor torques. It should be noticed that one of the main criteria for designing a gripper is its simplicity and robustness. Thus it is desired to provide the most effective grasping with the lowest amount of DOFs.

This goal is met in the present work while the UHVAT is an underactuated mechanism with a lot of motors. Two DOFs in open condition for each finger are considered for UHVAT. This mechanism and its related motors are considered in order to provide a grasping process with a complete encompass of the target object. In some cases, complete encompass is not necessary since the key factor which holds the object is the friction force and this force is depended on the normal force and the coefficient of friction. Thus at least two normal forces should act on the object from opposite sides. So, for a successful grasping, what matters is the friction force and the normal force and friction force is independent of the contact area. Therefore, two contact points with enough normal and friction are sufficient for a good grasping and holding. The mentioned considerations are investigated in this paper and the main factors for a firm grasping are discussed with details. The elegant aspect of the proposed gripper in this paper is that the reaction forces on the moving chassis

© 2021 IAU, Majlesi Branch

resulted from the gripper actuators are also controlled. In other words, the novelty of this paper is to compensate and control the mentioned phenomena while in the other relevant studies, the control operation is only focused on gripper's motion itself and the effect of these reaction forces is not considered. Also, the pivot point of applying the motor torque in UHVAT is supposed to be stationary and connected to the ground while here a more realistic model of a gripper is investigated in which the pivot point is located on the robot (the wrist point for the manipulating arm). Thus the mentioned corresponding reaction forces need to be neutralized using a proper controller. To illustrate the explained phenomena, during the design of a grip-based manipulator, this huge amount of force and torque which affect the manipulator link through the reaction torque from the gripper motors should be considered. This unwanted reaction torque deviates the gripper from its target and needs to be controlled on the arm motor (the motor which is connected to robot chassis) for a proper approach. Since the amount of these reaction torques are time-dependent and is not predictable, the best choice is to consider them as an external disturbance and their destructive effect should be neutralized by using a robust controlling strategy. For the proposed gripper in this paper, the above-mentioned consideration is inevitable and since this gripper is designed for high load applications, providing the accuracy and stability of its related manipulator is extremely significant. Since for a firm grasping, a huge amount of torque should be exerted to lock the gripper, its reaction torque from this actuator affects the related arm motion. Thus a strong robust nonlinear controller such sliding mode controller is required to compensate the mentioned manipulator disturbances. One of the main earliest studies related to control a mechanical arm using sliding mode was performed by Slotine [20].

This study is extended in [21] in which parametric uncertainties are also engaged in modeling and the controller is improved so that the chattering phenomenon is compensated. In another study, he delivered a stronger controller by combining the robustness of the sliding mode method with an adaptive algorithm through which not only the stability and accuracy could be guaranteed in a robust way, but also the uncertain parameters could be estimated too [22]. This adaptive sliding mode is also applied for a mechanical arm with flexible joints [23]. Here the adaptive algorithm is derived from the Lyapunov theory. The sliding mode can also be combined with PID method for a robotic system [24] which provides asymptotical stability for tracking control of an advanced robot using Lyapunov theory in which the experimental results from sliding mode method and simple PID method are compared. In [25], the sliding mode controller is strengthened using a compensator and the destructive effect of chattering is neutralized using an integrator parameter. The positive effect of this controller is verified by testing the controller on a MIMO (Multi-Input-Multi-Output) system.

The performance of sliding mode is extremely dependent on knowing the exact value of the uncertainty bounds. UDE (Uncertainty and Disturbance Estimator) method [26] provides an approach to decrease this sensitivity and provides the possibility of designing a sliding mode controller while it is not required to know the exact bound by using the measured values from the previous moments of operation. This method is an efficient solution whenever the variation of uncertainties is smooth. The main methods of designing a controller according to SMC (Sliding Mode Control) is introduced in [27-28] for the control engineers and its related challenges such as chattering, uncertainty bounds and etc. are explained.

It can be seen from the mentioned literature that, robust design of a stable gripper is ignored so far. The firm grasping of the gripper requires the static model of the system in order to check the slippage condition of the gripper. Also, some grippers introduced in literature have complicated structures with numerous DOFs and fingers which makes its control procedure difficult. Thus in this paper, a novel gripper mechanism is introduced and designed which has a simple mechanism and provides a good grasping force. Kinematics and statics of the gripper are extracted and its mechanism is optimized to provide a firm grasping for increasing the stability of the robot. The model is simulated and its results are verified by MATLAB-Simulink and also MSC_ADAMS. The fabrication procedure of the manufactured gripper is also explained and it is shown that this gripper meets the required expectancies and is firm enough to bear the total weight of a climbing robot. The mechanical arm which our proposed gripper is installed on is controlled by using the SMC method and its efficiency is verified by conducting some simulation scenarios in MATLAB-Simulink.

This effect of the gripper on its related arm is a novel study that is considered here while it was ignored in previous works. It will be shown that the proposed gripper installed on the manipulator which the arm motor is controlled by the designed sliding mode controller can successfully provide the required support for climbing the heavy robots through the pipe-shaped structures. In section two, the gripper design procedure is explained, in section three the modeling of the gripper is derived including kinematics, statics, and control strategy. Afterward in section four, fabrication of the designed gripper is explained and finally, in section five, modeling verification of the proposed gripper is performed by the aid of some simulation scenarios and their related analysis. Conclusion and discussion are explained in section six.

© 2021 IAU, Majlesi Branch

2 GRIPPER DESIGN

The designed gripper in this paper is a finger-shaped gripper which is suitable for grasping the circular and even semi-circular shape bars (or pipes). The main target toward designing this gripper is its high load capability and robustness against slippage during the time that reaction torques from main motors related to the climbing robot and weight force of the whole robot are exerting on grippers. The gripper should withstand these conditions to balance the climbing robot in height.

Another challenge that should be considered for designing the gripper is the good maneuverability and adaptability of the gripper such that the gripper can open wide enough and successfully encompasses the bar with a proper configuration and also its configuration should be simple enough for ease of control. Therefore, the mechanism of the proposed gripper is inspired by locking plier through which the mentioned required strength for locking a bar with no slippage possibility could be realized. The mechanism is modified as a two-finger gripper so that a motor would be able to open and lock the mentioned gripper using a one DOF additive mechanism. In "Fig. 1", the CAD model of the proposed gripper with its components is shown.

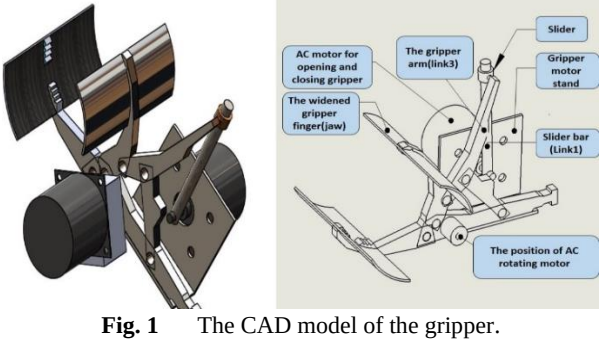

Fig. 1 The CAD model of the gripper.

It can be seen from "Fig. 1" that by rotation of the slider bar connected to the gripper lever using a revolute joint, the finger of the gripper rotates and consequently the grasping and releasing operation could be accomplished by rotation of the slider bar in CW or CCW directions. In other words, the mentioned slider is an interaction between the slider bar and the gripper lever which can move freely along the slider bar while the slider itself acts as a revolute joint through which the lever can rotate about it. By dividing the whole system into two subsystems, two 4-bar mechanisms (loop 1 and loop 2) appear which can be seen in "Fig. 2".

In "Fig. 2", the joints are shown by J1 to J7 in which J7 declares a prismatic joint for the above-mentioned slider. All moving links are shown by d1,d2,b1,b2, and C where d1 and d2 together configure the sliding bar. Actually, the slider is modeled as a passive prismatic joint. Employing Gruebler formula, the DOF of the system can be obtained as "Eq. (1)":

$$DOFs = 3\times(N_m - N_J) + N_J = 3\times(5-7)+7 = 1 \quad (1)$$

Where, N_m is the number of moving members (d1,d2,b1,b2, C) and N_J is the number of total DOFs of all of the joints, thus, N_J =7 and therefore, according to Gruebler formula defined in "Eq. (1)" one can conclude that the resultant DOF of the whole mechanism is one. It means that by using a motor as a rotary actuator, it is possible to lock and open the gripper mechanism.

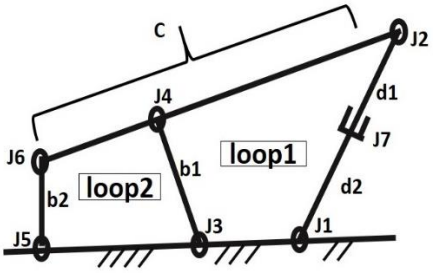

Fig. 2 Schematic of the gripper mechanism as 2 four-bar linkage.

This procedure is illustrated in "Fig. 3" in which the fingers of the gripper can be opened or closed by the rotation of the main joint as the controlling input of the mechanical motion.

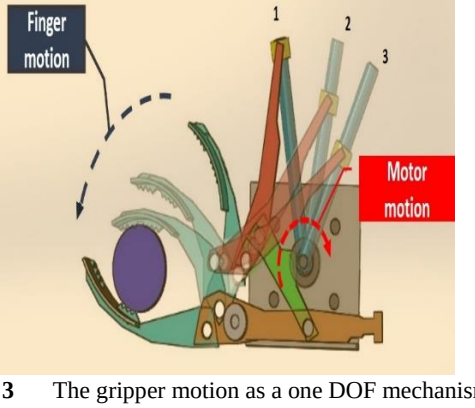

Fig. 3 The gripper motion as a one DOF mechanism.

3 MODELING

3.1. Kinematics Modeling

The schematic of the proposed gripper is illustrated as following "Fig. 4" which has two 4-bar linkage mechanisms. One of the engaged mechanisms has a link with variable length (link 1) which is treated as a passive prismatic joint.

© 2021 IAU, Majlesi Branch

As can be seen from the schematic view of the gripper mechanism in "Fig. 4", link 3 is common between the two mentioned sub-mechanisms and link 1 has variable length. It should be considered that the link a1-a2 is stationary which is connected to the robot manipulating arm. The motor is installed on the joint Θ_1. Here the kinematics of the proposed mechanism of the gripper is extracted and the relation between the angle Θ_1 and angular velocity ω_1 is calculated with respect to angles and velocities of the other gripper's components. This is a common method to calculate the kinematics of a system mechanism as it was also performed for UHVAT gripper [19]. For the first closed-loop kinematic chain, we have "Eq. (2)" according to the schematic view of the gripper shown in "Fig. 4":

$$S_1^{\,2} = d^{\,2} + a_1^{\,2} - 2.d.a_1\cos(\theta_1) = b_1^{\,2} + c_1^{\,2} - 2b_1c_1\cos(\Phi_1)$$
$$\Rightarrow \Phi_1 = \cos^{-1}\left(\frac{(b_1^{\,2} + c_1^{\,2} - S_1^{\,2})}{2b_1c_1}\right)$$
$$\theta_{21} = \sin^{-1}\left(\frac{d\,\sin(\theta_1)}{S_1}\right)$$
$$\theta_{22} = \sin^{-1}\left(\frac{c_1\sin(\Phi_1)}{S_1}\right) \Rightarrow \theta_2 = \theta_{21} + \theta_{22}$$
$$\theta_3 = \sin^{-1}\left(\frac{d\,\sin(\theta_1) - b_1\sin(\theta_2)}{c_1}\right) \tag{2}$$

Now the second closed-loop kinematic chain (second sub-mechanism) is considered which results in:

$$\theta_3 = \sin^{-1}\left(\frac{b_1\sin(\pi - \theta_2) - b_2\sin(\theta_f)}{c_2}\right)$$
$$S_2^{\,2} = b_1^{\,2} + a_2^{\,2} - 2b_1a_2\cos(\theta_2) = b_2^{\,2} + c_2^{\,2} - 2b_2c_2\cos(\Phi_2)$$
$$\Phi_1 = \cos^{-1}\left(\frac{(b_2^{\,2} + c_2^{\,2} - S_2^{\,2})}{2b_2c_2}\right)$$
$$\theta_{f1} = \sin^{-1}\left(\frac{b_1\sin(\pi - \theta_2)}{S_2}\right)$$
$$\theta_{f2} = \sin^{-1}\left(\frac{c_2\sin(\Phi_2)}{S_2}\right) \Rightarrow \theta_f = \theta_{f1} + \theta_{f_2} \tag{3}$$

All parameters are shown in "Fig. 4" which are geometric parameters of the gripper components like the joints angles and the lengths of the links. Here all of the kinematic parameters are calculated as a function of Θ_1 and d. As the link 3 is common in two mechanisms, by the same amount of Θ_3 which can be defined as two different functions and by solving these two functions with respect to d by the elimination of the length d, "Eq. (4)" can be extracted:

$$\theta_3(\mathrm{d},\theta_1) = \sin^{-1}\left(\frac{d\,\sin(\theta_1) - b_1\sin(\theta_2(\mathrm{d},\theta_1))}{c_1}\right)$$
$$= \sin^{-1}\left(\frac{b_1\sin(\pi - \theta_2(\mathrm{d},\theta_1)) - b_2\sin(\theta_f(\mathrm{d},\theta_1))}{c_2}\right)$$
$$F(\mathrm{d},\theta_1) - G(\mathrm{d},\theta_1) = 0$$
$$\Rightarrow d = H(\theta_1)$$
$$\Rightarrow \theta_2 = \Theta_2(\theta_1), \theta_3 = \Theta_3(\theta_1), \theta_f = \Theta_f(\theta_1) \tag{4}$$

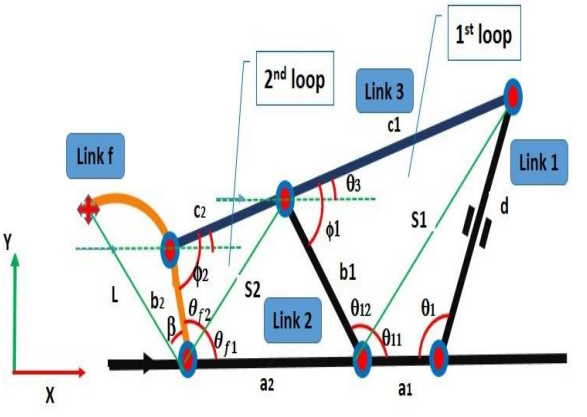

Fig. 4 The 2D schematic of grippers and geometrical parameters.

From "Eq. (4)", Θ_2, Θ_3, Θ_f, and d could be defined as the function of Θ_1 which can be shown as the functions $\Theta_2(\Theta_1)$, $\Theta_3(\Theta_1)$, $\Theta_f(\Theta_1)$, and $H(\Theta_1)$ in "Eq. (4)". For extracting the final formulation of the gripper kinematics, it is sufficient to provide the geometrical relations of the two mentioned closed-loop kinematic chains along with two directions of X and Y-directions. The velocity kinematics of the mechanism can also be extracted by the derivation of the above formulas with respect to time.

$$\mathrm{Xdir} \rightarrow \mathrm{b}_1\cos(\theta_2) + c_1\cos(\theta_3) + d\,\cos(\theta_1) = \mathrm{a}_1$$
$$\mathrm{Ydir} \rightarrow \mathrm{b}_1\sin(\theta_2) + c_1\sin(\theta_3) - d\,\sin(\theta_1) = 0$$
$$V_{Xdir} \rightarrow$$
$$-\mathrm{b}_1\omega_2\sin(\theta_2) - c_1\omega_3\sin(\theta_3) - d\,\omega_1\sin(\theta_1) + \dot{d}\,.\cos(\theta_1) = 0$$
$$V_{Xdir} \rightarrow$$
$$\mathrm{b}_1\omega_2\cos(\theta_2) + c_1\omega_3\cos(\theta_3) + d\,\omega_1\cos(\theta_1) + \dot{d}\sin(\theta_1) = 0 \tag{5}$$

The angular velocity of the second and third links as a function of Θ_1 and ω_1 can be derived by the velocity kinematics of the first closed-loop chain. The second and third links angular velocities are shown in "Eq. (6)" as functions of $\Omega_2(\Theta_1, \omega_1)$ and $\Omega_3(\Theta_1, \omega_1)$:

© 2021 IAU, Majlesi Branch

$$\omega_3 = -\frac{\left(\dot{d}\,.\cos(\theta_1+\theta_2) - \mathrm{d}.\omega_1.\sin(\theta_1+\theta_2)\right)}{c_1\sin(\theta_2-\theta_3)} = \Omega_3(\theta_1,\omega_1)$$
$$\omega_2 = \frac{\left(\mathrm{d}.\omega_1 - c_1.\omega_3\cos(\theta_1+\theta_2)\right)}{b_1\cos(\theta_1+\theta_2)} = \Omega_2(\theta_1,\omega_1) \quad (6)$$

Similarly, by solving the velocity kinematics of the second closed-loop kinematic chain, the angular velocity of the link F (the gripper finger) can be extracted as "Eq. (7)" which is a function of Θ_1 and ω_1 shown as $\Omega_f(\Theta_1, \omega_1)$

$$\omega_f = \left(\frac{b_1.\omega_2.\sin(\pi-\theta_2) - c_2\omega_3.\sin(\theta_3)}{b_2\sin(\theta_f)}\right) = \Omega_f(\theta_1,\omega_1) \quad (7)$$

Now it is possible to calculate the linear velocity of the endpoint of the gripper finger in two directions of X and Y shown as v_x and v_y in "Eq. (8)" as the functions $V_x(\Theta_1, \omega_1)$ and $V_y(\Theta_1, \omega_1)$:

$$v_x = L.\omega_f.\sin(\pi-\beta-\theta_f) = \mathrm{V}_x(\theta_1,\omega_1)$$
$$v_y = L.\omega_f.\cos(\pi-\beta-\theta_f) = \mathrm{V}_y(\theta_1,\omega_1) \quad (8)$$

The above equations declare the forward kinematics of the gripper which relates the joint space of DOF to the Cartesian workspace. In the simulation section, more analysis will be conducted to illustrate the gripper kinematics in more detail.

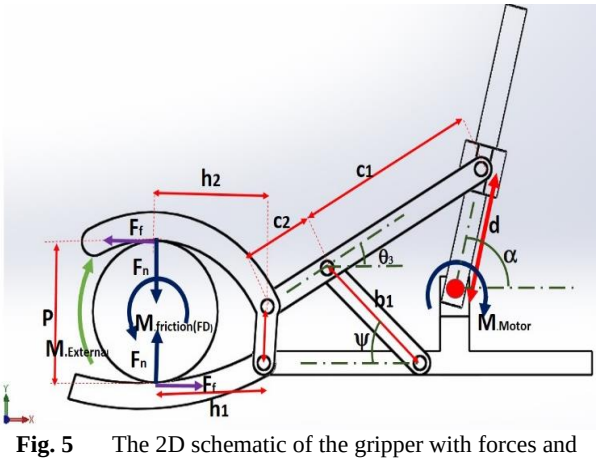

Fig. 5 The 2D schematic of the gripper with forces and torques acting on it.

3.2. Statics Modeling

As explained, the main objective of the proposed gripper design is to prevent it from slippage around the target pipe. Therefore, the calculation of the normal contact force and its corresponding friction force should be performed. The static formulations of the linkages are required to check the satisfaction of the explained non-slippage condition. The static friction force should be higher than the reaction friction force to guarantee the static equilibrium. In "Fig. 5", the geometric parameters are shown as the angles of components or the lengths of the links. Here we can see that a pipe with a diameter of P is grasped by the gripper while the gripper motor exerts torque M_m and external torque M_{ext} is implemented from the environment.

When the gripper is in the locked configuration, the slide bar has the angle of α with the length of d which declares the position of gripper's motor. First, the free body diagram of links A, B, C, D, and E are extracted as following "Fig. 6".

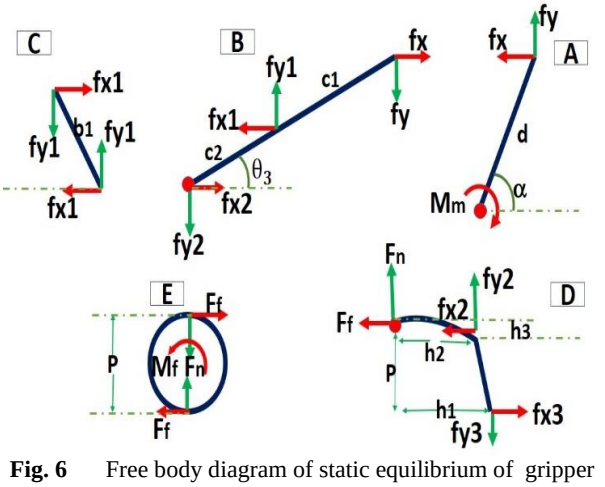

Fig. 6 Free body diagram of static equilibrium of gripper components.

Equilibrium equations of the related links can be written as "Eq. (9)":

$$A \rightarrow$$
$$f_x = M_m\sin(\alpha), f_y = M_m\cos(\alpha)$$
$$B \rightarrow$$
$$-f_{x1}+f_{x2}+f_x = 0, f_{y1}-f_{y2}-f_y = 0$$
$$f_x(\mathrm{c}_1+\mathrm{c}_2)\sin(\theta_3)+f_y(\mathrm{c}_1+\mathrm{c}_2)\cos(\theta_3) \quad (9)$$
$$-f_{y1}\mathrm{c}_2\cos(\theta_3)-f_{x1}\mathrm{c}_2\sin(\theta_3) = 0$$
$$C \rightarrow f_{x1}\tan(\psi)-f_{y1} = 0$$
$$D \rightarrow f_{x3}-f_{x2}-F_f = 0, -f_{y3}+f_{y2}+f_{y4} = 0$$
$$-f_{x3}P+f_{y3}h_1-f_{y2}h_2+f_{x2}h_3 = 0$$
$$E \rightarrow M_{ext}-F_f P = 0$$

Where, f_x, f_y, f_{x1}, f_{y1}, f_{x2}, f_{y2}, f_{x3}, f_{y3}, f_{y4}, M_{ext}, and F_f are joints generalized forces, contact and friction forces, M_m is the motor torque and M_{ext} is the external implemented torque from environment on the gripper. Thus here we

© 2021 IAU, Majlesi Branch

have a simultaneous set of ten equations with ten unknowns. Therefore, the contact force $F_n=f_{y4}$ can be calculated as a function of M_m, M_{ext},α, and d in "Eq. (10)":

$$F_n = f_{y4} = F(\mathrm{d}, \alpha, \mathrm{M}_m, \mathrm{M}_{ext}) \tag{10}$$

It should be considered that the above formulation is valid for the equilibrium condition. In other words, it is supposed here that the gripper does not slip and the static friction is more than the required friction which is exerted as the reaction torques from climbing robot's main motors. Following condition in "Eq. (11)" is required to satisfy the mentioned situation for equilibrium:

$$F_f < F_n \mu_s \Rightarrow F_f = \frac{M_{ext}}{P} \tag{11}$$

Where, μ_s is the coefficient of static friction. Since this gripper is supposed to bear the climbing robot weight, the rotational stability of the robot around all of the local axis should be provided.

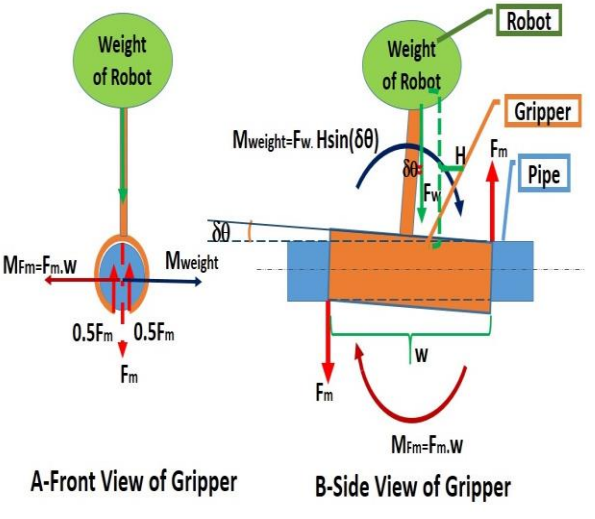

Fig. 7 The equilibrium diagram of the gripper from the side view.

The rotational stability of the robot around the grasped pipe axis can be guaranteed by providing sufficient contact area, however, if the center of mass of the robot would not be located within the plane of the robot (the robot tilts), the rotational equilibrium of the robot around the other axis could be violated. To cover the mentioned challenge, the finger width is broadened so that an opposite torque will be generated (M_{Fm}) during the moments that the robot is in the threshold of tipping over. So the contact forces (F_m) will be generated at the ends of the gripper finger as the required reaction forces. This torque can neutralize the created torque (M_{weight}) resulted from the weight of the robot so the robot falling will not occur. This modification in design is shown in "Fig. 7". As can be seen from "Fig. 7", when the robot tilts about δΘ, the weight of the robot F_w causes a tip over torque equal to M_{weight} which results in instability of the robot. By the aid of the mentioned remedy in gripper design, the reaction forces F_m created from the end sides of the gripper for the case of tipping over of the robot, an opposite torque (couple) is provided which neutralizes the effect of the mentioned tip over-torque.

3.3. Control Modeling

As mentioned, the proposed gripper is designed to grasp the pipes with a high contact force so that the weight of the climbing robot would be tolerated and the non-slippage condition is guaranteed. Thus the motor of the gripper would produce a considerable torque (M_m) which consequently results in huge contact force at the gripper finger. The reaction of this torque (gripper open-close motor) together with the torque which rotates the gripper (the gripper wrist motor) are variable and are not precisely predetermined. Thus this summation of torques (the reaction torques from gripper motors) will be implemented on the mechanical arm as an external disturbing torque and effects the rotational movement of the manipulating arm.

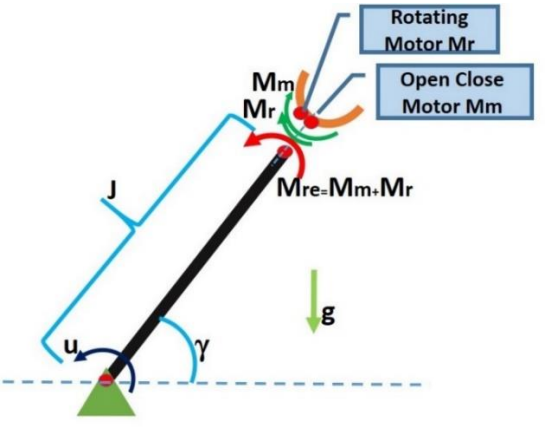

Fig. 8 Free body diagram of the robot arm and its implemented gripper.

Thus the motor related to this mechanical arm should be controlled in a robust way to compensate for the mentioned destructive disturbance. In fact, this subject is a novel study to investigate the effect of gripper's motors on the related arm. Previous studies are focused only on the gripper motion like the control strategy performed for UHVAT [19], but here in this paper, the related mechanical arm is also modeled to investigate the effect of the gripper's motors reaction forces on the robot. As the mechanical arm has a nonlinear equation of motion, so the nonlinear control method should be

© 2021 IAU, Majlesi Branch

employed such as sliding mode control which is a robust nonlinear controller. The aspect of these reaction torques which are exerting on robot arm manipulator is illustrated in "Fig. 8".In "Fig. 8", the summation of the grasping torque (M_m) and rotating torque (M_r) related to the gripper motors is shown by M_{re} which is considered as an external disturbance implementing on the arm. To compensate the destructive effect of these torques, the sliding mode controller is designed in this paper. Here, the effect of gripper's motor reaction forces is investigated on the robotic arm. Thus, the behavior of the robotic arm motion is supposed to be studied as a non-linear system for which the dynamic equation of the arm should be extracted and the reaction force of the gripper's motors should be considered as its related disturbances. The dynamic equation of the arm equipped by the designed gripper is as "Eq. (12)" which is a nonlinear equation of motion:

$$u = D\ddot{\gamma} + G(\gamma) + M_{re} \tag{12}$$

Where, Υ is the rotational angle of the arm, D is the inertia of the link, G is gravity vector ($G(\Upsilon)=5.88.\cos(\Upsilon)$) and M_{re} is the mentioned disturbance and u is the control input. The error of tracking can be defined as "Eq. (13)":

$$\tilde{\gamma} = \gamma - \gamma_d \tag{13}$$

Here Υ_d is the desired angle of the arm and $\tilde{\Upsilon}$ is the error of tracking. The sliding surface s can be defined as following "Eqs. (14), (21)":

$$s = \dot{\tilde{\gamma}} + \lambda\tilde{\gamma} \Rightarrow \dot{s} = \ddot{\tilde{\gamma}} + \lambda\dot{\tilde{\gamma}} = \ddot{\gamma} - \ddot{\gamma}_d + \lambda\dot{\tilde{\gamma}} \tag{14}$$

Where, λ is a positive definite constant and s=s(t) is a time-varying sliding surface. By substituting the dynamic equation from "Eq. (12)" into "Eq.(14)", the derivative of sliding surface (ṡ) can be rewritten as "Eq. (15)":

$$\dot{s} = \frac{u - G(\gamma) - \mathrm{M}_{re}}{D} - \ddot{y}_d + \lambda\dot{\tilde{\gamma}} \tag{15}$$

Two modes should be considered in sliding mode, reaching mode and tracking on slipping surface mode. First of all the controlling input should be calculated so that the states would converge to the sliding surface and in order to meet this goal ṡ should converge to zero, thus, the corresponding controlling input as the reaching mode control input can be extracted as "Eq. (16)":

$$\dot{s} = 0 \Rightarrow \hat{u} = D\left(\ddot{\gamma}_d - \lambda\dot{\tilde{\gamma}}\right) + G(\gamma) + \hat{\mathrm{M}}_{re} \tag{16}$$

Here û is the controlling input related to reaching mode and $\hat{\mathrm{M}}$ is initially uncertainty guess which is the implemented disturbance on the robotic arm. Now the following control law introduced in "Eq. (17)" can be defined in a way that both of reaching and tracking modes can be covered simultaneously:

$$Control\_Law \rightarrow u = \hat{u} - K.\mathrm{sgn(s)} \tag{17}$$

At the above formula in "Eq. (17)", a switching function(sgn(s)) is considered so that the tracking error can converge to zero. To meet this goal, the controlling gain of K (switching coefficient) should be calculated properly. If the following condition in "Eq. (18)" is satisfied then the tracking condition can be guaranteed:

$$\frac{1}{2}\frac{d}{dt}s^2 \le -\eta|\mathrm{s}| \Rightarrow \mathrm{s}\dot{\mathrm{s}} \le -\eta|\mathrm{s}| \tag{18}$$

In "Eq. (18)", η is a positive definite value. As seen, to satisfy the convergence condition for s toward zero, the above condition in "Eq. (18)" should be satisfied which declares the Lyapunov stability theorem. Now ṡ which was derived from "Eq. (15)" should be substituted to the "Eq. (18)". Then one can conclude "Eq. (19)":

$$\mathrm{s}\left(\frac{u - G(\gamma) - \mathrm{M}_{re}}{D} - \ddot{\gamma}_d + \lambda\dot{\tilde{\gamma}}\right) \le -\eta|\mathrm{s}| \tag{19}$$

By substituting the finalized controlling input from "Eq. (17)" instead of u in "Eqs. (19), (20)" can be obtained:

$$\mathrm{s}\left(\frac{\hat{u} - K.\mathrm{sgn(s)} - G(\gamma) - \mathrm{M}_{re}}{D} - \ddot{\gamma}_d + \lambda\dot{\tilde{\gamma}}\right) \le -\eta|\mathrm{s}| \tag{20}$$

Finally, the following formula as "Eq. (21)" can be extracted by substituting the û from "Eq. (16)" into "Eq. (20)":

$$\mathrm{s}\left(\frac{D\left(\ddot{\gamma}_d - \lambda\dot{\tilde{\gamma}}\right) + G(\gamma) + \hat{\mathrm{M}}_{re} - K.\mathrm{sgn(s)} - G(\gamma) - \mathrm{M}_{re}}{D} - \ddot{\gamma}_d + \lambda\dot{\tilde{\gamma}}\right) \le -\eta|\mathrm{s}| \tag{21}$$

Summarizing the above equation to "Eq. (22)" results in choosing the proper gain of K by which the value s can converge to zero:

© 2021 IAU, Majlesi Branch

$$s(\text{sgn}(s)) = |s| \Rightarrow s\left(\hat{M}_{re} - M_{re}\right) - K|s| \le -\eta D|s|$$
$$\Rightarrow K \ge |\hat{M}_{re} - M_{re}| + \eta D \quad (22)$$

Thus, the controlling input can be improved as "Eq. (23)" by substituting the calculated switching gain:

$$u = \hat{u} - \left(|\hat{M}_{re} - M_{re}| + \eta D\right).\text{sgn}(s) \quad (23)$$

Here in "Eq. (23)", $|\widehat{M_{re}} - M_{re}|$ is bound of uncertainty (unknown disturbance). In order to decrease the effect of chattering phenomena following modification as "Eq. (24)" can be considered instead of switching function [28]:

$$\text{sgn}(s) = sat\left(\frac{s}{\Phi}\right) \Rightarrow u = \hat{u} - \left(|\hat{M} - M| + \eta D\right).\text{sat}\left(\frac{s}{\Phi}\right) \quad (24)$$

Where ϕ is the thickness of the boundary layer around the sliding surface s and instead of sgn function which is a totally discontinuous function, the saturation function (sat) is used so the high-frequency chattering problem can be resolved by employing "Eq. (24)". According to the above-designed controller, the arm equipped by the designed gripper can be successfully controlled in the presence of the gripper motor's reaction torque exerting on the mechanical robot arm (disturbances).

4 FABRICATION

The main actuator for open-closing the gripper is a 220 volts AC motor which can generate 8 N.m torque with the angular velocity of 1.2 revolutions per minute. When grasping condition is accomplished, the gripper locks on the pipe by a locking toggle which does not let the gripper open suddenly and by consideration of high ratio gearbox implemented on AC motor, back drivability for the mentioned actuator is prevented to ensure when the electricity is gone the locking condition continues. So the mechanical locking process is provided for the designed gripper. Another motor just like the mentioned one for open-closing the gripper is chosen to rotate the gripper to align the gripper on the target pipe(wrist motor). To control open-closing or rotating operation, some DC two-channels relays are employed which are controlled by main Arduino microcontroller in which by signals coming from Arduino the relay opens one circuit (e.g. CW rotation of AC motor) and closes the other circuit (e.g. CCW rotation of AC motor). The employed slider is to open-close the gripper and it is made of phosphor bronze material which can slide easily with low friction on the slide bar (link A) connected to the open-close motor and also it is a frictionless joint which connects links A and B (look at the illustrating "Fig. 1"). For gripper's jaws, the widened structure is attached to the fingers with dry soft rubber covering the inside surface to fill all possible gaps between the pipe and gripper's jaws ("Fig. 1") and the middle area of the grippe's jaw is teeth-shaped for providing the highest static friction coefficient.

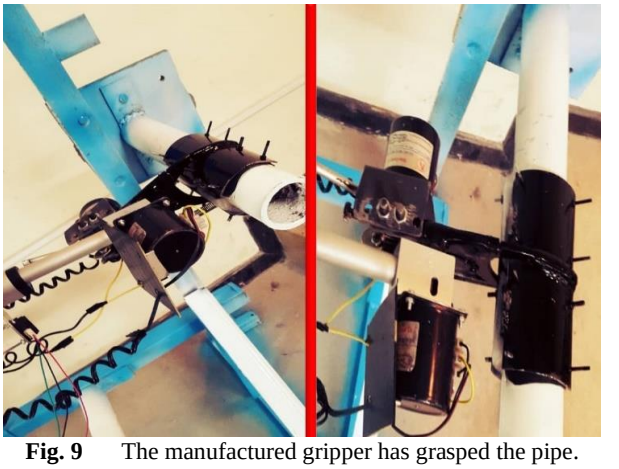

Fig. 9 The manufactured gripper has grasped the pipe.

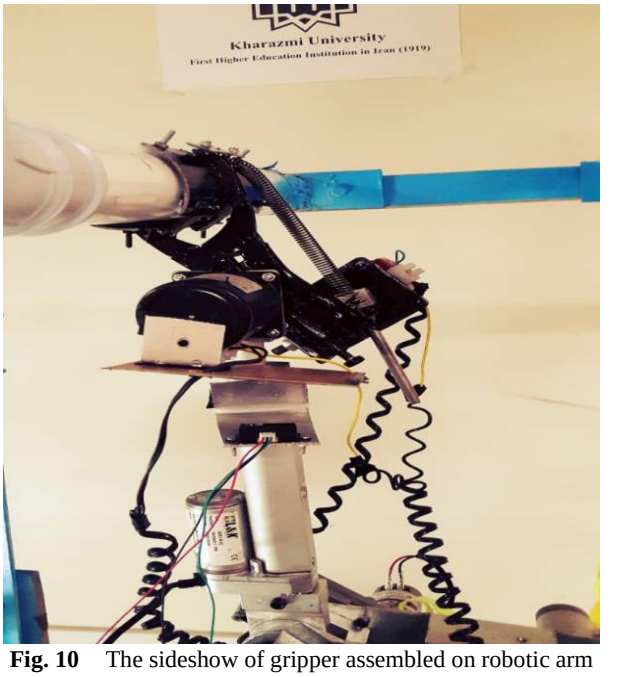

Fig. 10 The sideshow of gripper assembled on robotic arm manipulator.

The whole mechanism is connected to the climbing robot's manipulating arm which is driven by a 24volts DC motor with a maximum torque of 17.6 N.m. This DC motor which is related to the robotic arm is supposed to be controlled in this paper by the 600 pulse A/B encoder

© 2021 IAU, Majlesi Branch

attached to the rotating shaft of the motor. In "Fig. 9", a prototype of the gripper is shown which has grasped the pipe.In "Fig. 10", the gripper which is assembled on the robotic arm is shown grasping the target pipe firmly.
In "Fig. 11", it can be observed that the total weight of the robot is tolerated by two grippers which are grasping two pipes that are treated as the main support for the whole 20Kg climbing robot in which the proposed gripper is designed to perform such this specific desired application:

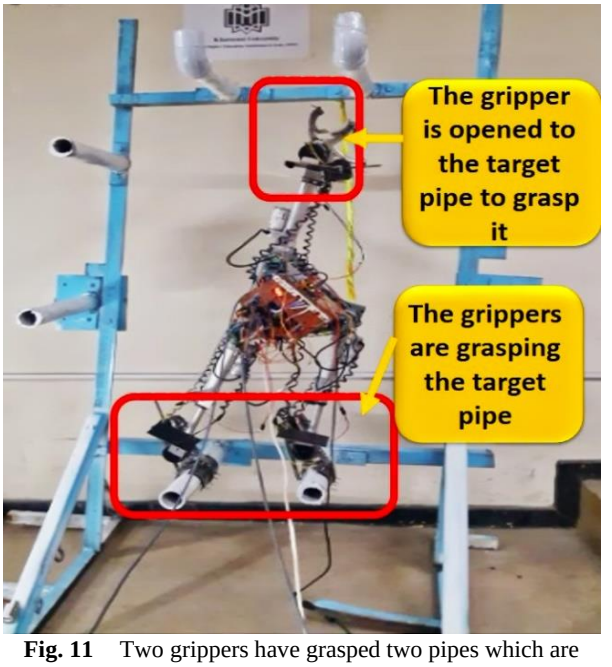

Fig. 11 Two grippers have grasped two pipes which are treated as firm support of whole 20Kg climbing robot.

5 SIMULATION

5.1. Kinematics Simulation

The gripper is a one DOF mechanism in which its kinematic equations were derived using geometric relations extracted in "Eqs .(6), (7)" so all of the joints' angles and velocities can be obtained according to the angular position (θ_1) and angular velocity of the main DOF (ω_1). Therefore, the results of "Eqs .(6), (7)" are shown in "Figs. 12, 13 and 14" for a specific motion defined by "Eq. (25)" for 6 seconds back and forth motion of the main DOF, which the kinematics calculation results are compared with MSC-ADAMS simulation results:

$$\omega_1(t) = \frac{\pi}{10.2}\cos(\frac{\pi}{6}t) \tag{25}$$

The angular velocities of gripper's components ω_2, ω_3, and ω_f are shown in "Figs. 12, 13 and 14" for the desired motion defined as "Eq. (25)" for the main DOF. The simulation process is according to the Table of the list of parameters provided in the last section of the paper. As can be seen from the above diagrams, there is great compatibility between MATLAB results from the kinematic calculation and MSC-ADAMS simulation for all of the three main gripper components (link2, link3, link f) which indicates the correctness of kinematic calculation from kinematics section.

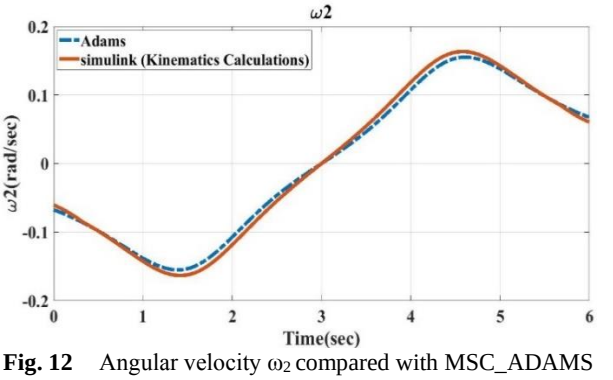

Fig. 12 Angular velocity ω_2 compared with MSC_ADAMS simulation result.

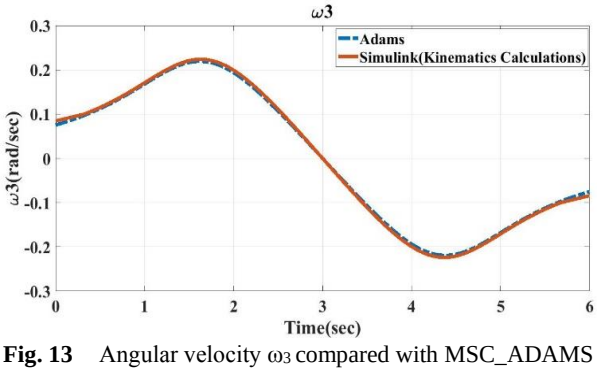

Fig. 13 Angular velocity ω_3 compared with MSC_ADAMS simulation result.

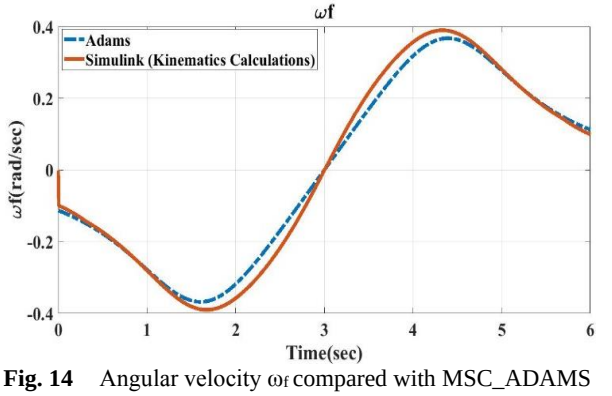

Fig. 14 Angular velocity ω_f compared with MSC_ADAMS simulation result.

In "Fig. 15", the comparison between the main DOF angular velocity (ω_1) and the finger's angular velocity (ω_f) is shown. It is obvious that at the start and endpoint of the gripper motion when the figures touch the pipe, the angular velocity of the finger is about 1/3 of the main

© 2021 IAU, Majlesi Branch

DOF angular velocity which means that in grasping phase the finger moves gently without any shock or tough impact on the target pipe so in grasping phase with slow angular velocity of finger, the pressing process occurs. Now the forward kinematics is investigated and its results are compared with MSC-ADAMS simulation results which this comparison is shown in "Fig. 16" for both directions of X and Y for horizontal and vertical displacements values of the finger.

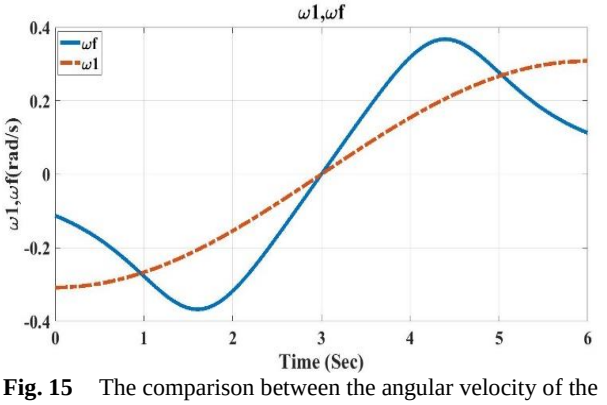

Fig. 15 The comparison between the angular velocity of the main DOF (ω_1) and the finger angular velocity (ω_f).

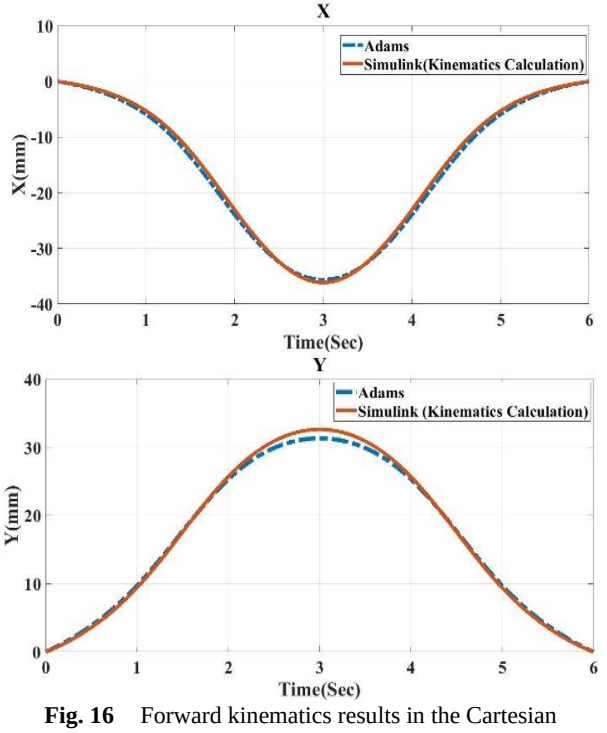

Fig. 16 Forward kinematics results in the Cartesian workspace and its comparison with MSC-Adams along X and Y direction.

As can be seen from "Fig. 16", for closing and opening modes of the gripper, a back and forth motion of the finger in the Cartesian workspace can be observed. Good compatibility between MATLAB and MSC-ADAMS shows the correctness of the extracted modeling. In the end, all of the kinematic responses of other components of the gripper can be obtained by the aid of the calculated motor angle according to the kinematic model obtained from equations in the kinematic section of this paper.

5.2. Statics Simulation

As mentioned in the static section, for a proper grasping with no slippage, the normal force of the gripper should be increased as high as possible so the static friction force can be increased. This force is a function of gripper's configuration in its closed state, the amount of external torque, the length d, and the angle α which was derived in statics section.

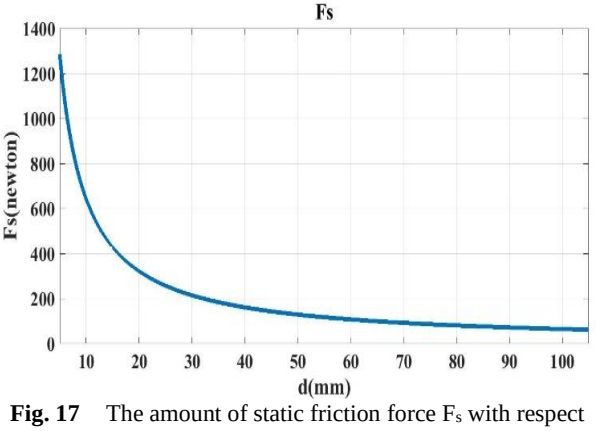

Fig. 17 The amount of static friction force F_s with respect to distance d.

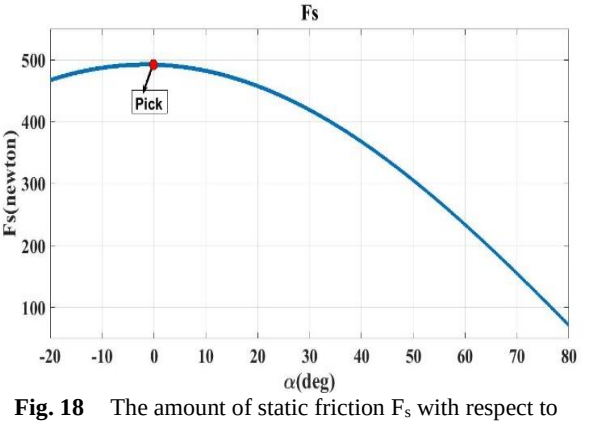

Fig. 18 The amount of static friction F_s with respect to angle α.

In fact, the length d and the angle α indicate the gripper open-close motor position and this means that the amount of the normal force is the function of the gripper's motor position. So, according to static force function in "Eq. (10)", the static force (F_s) is a function of d and α and these dependencies are shown in "Figs. 17, 18" as the diagrams which show how static friction force changes with respect to d and α magnitudes by considering no external torque (M_{ext}=0). The same comparison is also conducted by considering the

© 2021 IAU, Majlesi Branch

constant torque of 8 N.m for gripper's motor (M_m=8 N.m) and static friction coefficient of 0.5 between the pipe and gripper's finger. Therefore, if the reaction friction force between the finger and pipe would be lower than the static friction force, the non-slipping condition is guaranteed.

As can be seen from "Fig. 17", by constant value α=0.82 rad, by increasing the length d, the value of F_s decreases homographically. Now the F_s relations with angle α is extracted considering d=5mm which is shown in "Fig. 18". It can be seen from "Fig. 18", when the angle increases from a negative value to positive, the static friction increases until the angle α equals to zero. Afterward, F_s decreases as the angle increases. It can be concluded that the growth of F_s according to angle α is harmonic. Also it can be seen that, the maximum F_s has occurred in α=0 and d=0 but the manufacturing limitations do not permit this values for design process since by decreasing the length d, the reaction force on critical joints such as slider joint increases extremely which can cause joint failure by extreme stress which would be caused from that huge force on the mentioned joint. Considering the manufacturing limitation we know that the least size of length d and angle α in grasping state configuration is the best choice to achieve large static friction forces. Now by considering values of 20 mm and 0.82 rad for the distance d and angle α for the grasping phase, the comparison between the static friction force and reaction friction force with respect to the external torque (M_{ext}) according to the "Eq. (10)" are illustrated in "Figs. 19, 20" for two directions of external torque. We know that for the non-slippage condition the reaction friction force (F_f) should be less than static friction force (F_s).

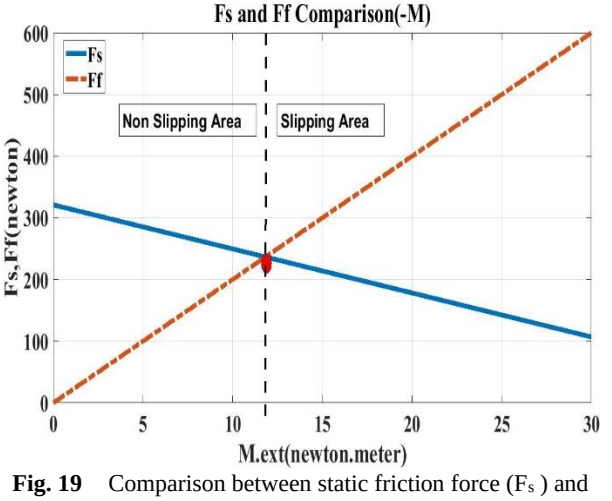

Fig. 19 Comparison between static friction force (F_s) and reaction friction force (F_f) by increasing the absolute amount of external torque (M_{ext}) with negative values.

From "Fig. 19", it can be observed that for the negative values of external torque(M_{ext}), the reaction friction force (F_f) increases linearly and the value of static friction force (F_s) decreases linearly as the absolute value M_{ext} increases from zero and this procedure continues. The intersection of these two profiles is at M_{ext}=12 N.m which is the slippage threshold point. Therefore, for the negative values of M_{ext} which their absolute values are less than 12 N.m, the safe zone for the non-slipping condition is M_{ext}<12 N.m. Now the positive values of M_{ext} are investigated in "Fig. 20".

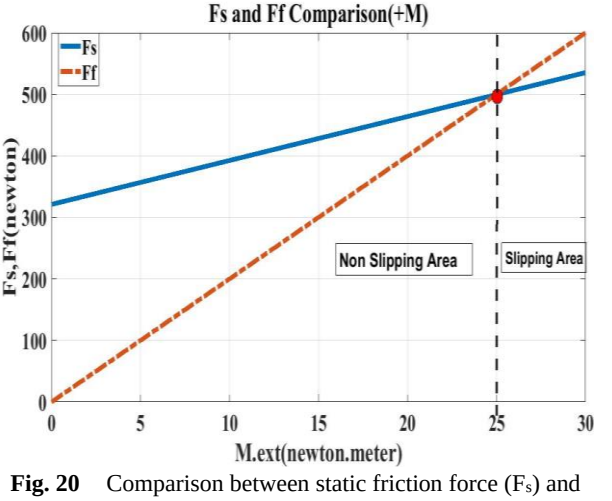

Fig. 20 Comparison between static friction force (F_s) and reaction friction force (F_f)by increasing the absolute amount of external torque (M_{ext}) with positive values.

From "Fig. 20", it can be concluded that for the positive values of M_{ext} ,by increasing M_{ext} from zero, the F_s and F_f increase linearly with different slope angle and the intersection of the profiles is at the value of 25 N.m for M_{ext}. Therefore, the values less than 25 N.m for positive direction of M_{ext} are in the safe non-slipping zone which is a wider area than the safe area obtained for the negative direction of M_{ext}. By increasing the static coefficient (μ_s) and decreasing the value of length d and angle α as a result of the mentioned manufacturing limitations, the bounds of the extracted safe non-slipping zones for both directions of M_{ext} increase which consequently increases the factor of safety for the non-slipping condition.

5.3. Control Simulation

In this part, the efficiency of the designed controller is verified by conducting some simulation scenarios. As it was explained we suppose that the reaction torque of gripper's motors is applied on the arm motor which is considered as a disturbance. Here this disturbance is supposed as "Eq. (26)" in the actual state for 10 seconds of arm motion:

$$M_{re} = 25\cos(t)(\text{newton}.\text{meter}) \quad (26)$$

The related bound of disturbance M_{re}, is about 30 N.m. We consider the initial error 0.5 rad for the arm angle

© 2021 IAU, Majlesi Branch

and so both the regulation and tracking control should be accomplished by the designed sliding mode controller. The desired path for angle Υ is chosen as "Eq. (27)" which is a function of time for 10 seconds of arm motion:

$$\gamma = 2.\sin(0.2\,t)(rad) \tag{27}$$

As was explained in the control section, the sliding mode controller suffers from the chattering effect. According to "Eq. (24)", with consideration of bound ϕ=0.1 for the sliding surface boundary layer and saturation function, a smooth response (continuous) can be achieved. The SMC coefficients of λ and η, are chosen about 15 while the inertia parameter (D) is 0.165 and the gravity coefficient is 5.88 according to the robot's arm mass and length. Therefore, according to SMC method, control error for a smooth response (bound of sliding surface ϕ=0.1) and chattering response (switching sign function) are compared and shown in "Fig. 21".

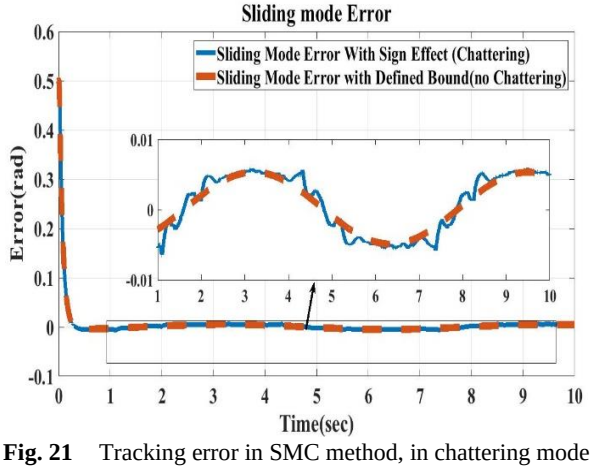

Fig. 21 Tracking error in SMC method, in chattering mode (switching sign function) and smooth mode (saturation function with bound of ϕ.

The corresponding comparison related to the inputs of these two simulations is shown in "Fig. 22".

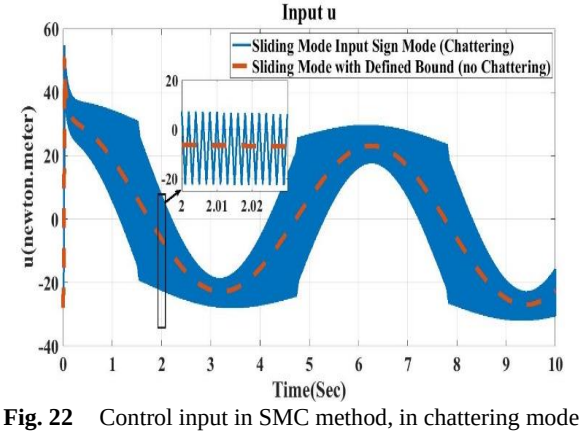

Fig. 22 Control input in SMC method, in chattering mode (switching sign function) and smooth mode (saturation function with bound of ϕ).

From "Fig. 21" it can be observed that the error converges to zero by the SMC method for both approaches. In "Fig. 22", it is observed that in sign function mode SMC, the inputs oscillates intensely between 10 and -20 N.m which is not desirable control input while in the improved approach with bound of ϕ=0.1, the unwanted chattering phenomena is eliminated and the continuous response has resulted. The PD controller is also compared with the improved SMC considering bound of ϕ=0.1. For PD controller, the gains of Kp=100 and Kv=50 are set based on the pole placement method. By increasing the gains, tracking precision will be increased while it can also motivate the unmolded natural frequencies and results in instability [29]. Thus to illustrate the superiority of the SMC, the comparison is provided with PD controller with high gains which are extremely larger than SMC control coefficients (about 15). In "Eq. (28)" the formulation of PD controller is defined:

$$u = Kp.e + Kv.\dot{e} \tag{28}$$

As can be seen, the input control law is a linear equation of error (e) and its derivative ($\dot{e}$) with proportional gain Kp and derivative gain of Kv. In "Fig. 23", the comparison of the actual path employing the two mentioned controlling strategies with respect to the desired path (defined in "Eq. (27")), is demonstrated with 0.5 rad initial error. This initial condition is to engage the regulation process of the controllers in the presence of disturbance M_{re}.

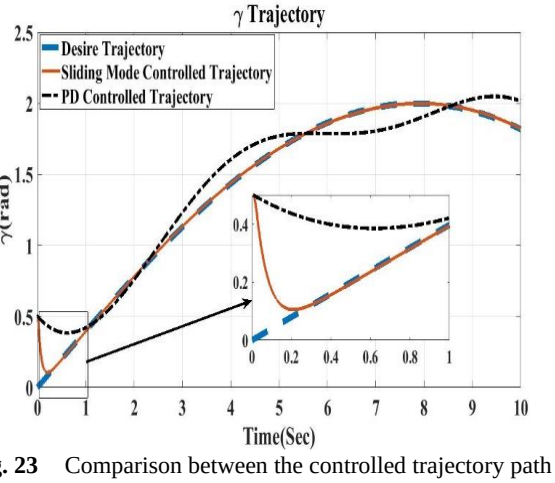

Fig. 23 Comparison between the controlled trajectory path by sliding mode and PD controller.

According to "Fig. 23", it can be concluded that the desired path is precisely tracked by the SMC method while PD response has considerable deviation with respect to the desired trajectory. In "Fig. 24", the error comparison of these two controllers is shown accordingly to clarify the superiority of SMC rather than PD controller.

© 2021 IAU, Majlesi Branch

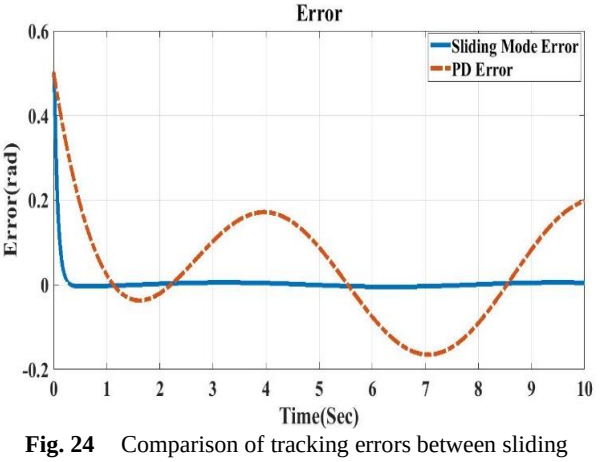

Fig. 24 Comparison of tracking errors between sliding mode and PD controller.

As can be seen from "Fig. 24", the error of the SMC method converges to zero in less than 0.2 seconds which is a fast response, while PD error oscillates around zero with a considerable domain. So the arm follows the desired path in less than 0.2 seconds in the presence of disturbances caused by the gripper's motor reaction forces. Considering the fact that during grasping the pipes by the designed grippers, the robot mechanism converts to a closed-kinematic chain, the precision is extremely significant and any error is destructive since it can result in system collapse. Thus, it can be concluded that the designed SMC controller is extremely necessary for covering the grasping process of climbing robots which are equipped by the proposed gripper that the reaction torques from their motors (gripper motors) can be exerted on the robot arm as considerable disturbances which their effect should be repelled by a robust controller, for example sliding mode controller proposed in this paper.

6 CONCLUSION

In this paper, a novel gripper with a novel mechanism is proposed and manufactured by which a high amount of load and torque can be tolerated without any slippage. This gripper is extremely applicable for grip-based manipulator especially for the climbing robots in which the load of the robot needs to be tolerated. The kinematics of the gripper were calculated by which the required angular velocity of the input motor can be estimated to accomplish the opening and locking process of the gripper jaw. Afterward, the quasi-static analysis of the proposed gripper was extracted by which the required motor torque can be calculated for a robust grasping. It was explained that in order to increase the safety factor related to the non-slippage condition, it is required to increase the static friction force of the jaw then an analysis study was performed in which the optimum values of the geometrical configuration of the gripper were estimated. It was shown that this critical normal force is a function of the motor torque, the position of the motor, and the external implemented torque on the gripper caused by robot's weight or etc. It was concluded that the less the distance of d and the angle of the α, the more the static friction force results accordingly. However, as was explained, due to manufacturing limitations, the minimum amount of 20 mm for distance d and 0 degrees for α were applicable practically. Also, the maximum toleratable external torque capacity of the gripper was extracted for both directions and the corresponding safe zone of the designed gripper for the non-slippage condition was analyzed as a function of the mentioned parameters. It was seen that the maximum tolerable torque of the gripper in the clockwise direction is about 25 N.m while this value is about 12 N.m for counter-clockwise direction. Finally, in order to compensate the destructive effect of external torque resulted from the robot dynamic in climbing process, a robust controller named SMC was designed and implemented on the arm's motor of the robot to neutralize the implemented disturbances from the gripper's motor torque reactions. The performance of the designed robust controller was compared with a simple PD controller and it was shown that by employing the designed SMC controller, the settling time of tracking operation is about 0.2 sec while using a simple PD, the system remains in the border of instability. The performance of the proposed gripper and its optimization analysis were performed by conducting some simulation in MATLAB-Simulink and the corresponding results were verified by MSC-ADAMAS. Also, the efficiency of the designed robust controller was investigated by comparing the performance of the manipulator with a simple linear controller. It was shown that using the proposed gripper equipped by the designed nonlinear controller, it is possible to accomplish a climbing procedure for an ascending robot with accurate positioning.

7 LIST OF PHYSICAL PARAMETERS

Physical properties of the system

Symbol	Value	Definition	Unit
c_1	85.3	Geometric parameter in Fig.4	mm
c_2	33.2	Geometric parameter in Fig.4	mm
L	60.86	Geometric parameter in Fig.4	mm
b_1	60.21	Geometric parameter in Fig.4	mm
b_2	24.52	Geometric parameter in Fig.4	mm

© 2021 IAU, Majlesi Branch

a_1	36.91	Geometric parameter in Fig.4	mm
a_2	75.12	Geometric parameter in Fig.4	mm
h_1	70.26	Geometric parameter in Fig.5	mm
h_2	50.34	Geometric parameter in Fig.5	mm
h_3	4.14	Geometric parameter in Fig.6	mm
P	50	Pipe diameter	mm
ψ	0.5	Geometric parameter in Fig.5	rad
μ_s	0.5	Static friction coeficient	-
g	9.8	Gravity accelration	$\frac{m}{s^2}$
w	300	Gripper width	mm

REFERENCES

[1] Zhang, J., Fang, X., Challenges and Key Technologies in Robotic Cell Layout Design and Optimization, Proceedings of the Institution of Mechanical Engineers, Part C, Journal of Mechanical Engineering Science, Vol. 231, No. 15, 2017, pp. 2912-24.

[2] Bicchi, A., Hands for Dexterous Manipulation and Robust Grasping: a Difficult Road Toward Simplicity, IEEE Transactions on Robotics and Automation, Vol. 16, No. 6, 2000, pp. 652-62.

[3] Hsu, J., Yoshida, E., Harada, K., and Kheddar, A., Editors., Self-Locking Underactuated Mechanism for Robotic Gripper, 2017 IEEE International Conference on Advanced Intelligent Mechatronics (AIM), 2017, IEEE.

[4] Rojas, N., Ma, R. R., and Dollar, A. M., The GR2 Gripper: an Underactuated Hand for Open-Loop in-Hand Planar Manipulation, IEEE Transactions on Robotics, Vol. 32, No. 3, 2016, pp. 763-70.

[5] Puig, J. E. P., Rodriguez, N. E. N., and Ceccarelli, M., A Methodology for the Design of Robotic Hands with Multiple Fingers, International Journal of Advanced Robotic Systems, Vol. 5, No. 2, 2008, pp. 1-22.

[6] Choi, M. S., Lee, D. H., Park, H., Kim, Y. J., Jang, G. R, and Shin, Y. D., et al., Editors., Development of Multi-Purpose Universal Gripper, 2017 56th Annual Conference of the Society of Instrument and Control Engineers of Japan (SICE), 2017, IEEE.

[7] Takaki, T., Omata, T., High-Performance Anthropomorphic Robot Hand with Grasping-Force-Magnification Mechanism, IEEE/ASME Transactions on Mechatronics, Vol. 16, No. 3, 2010, pp. 583-91.

[8] Liu, C. H., Chiu, C. H., Editors., Design and Prototype of Monolithic Compliant Grippers for Adaptive Grasping, 2018 3rd International Conference on Control and Robotics Engineering (ICCRE), 2018, IEEE.

[9] Yi, B. J., Na, H. Y., Lee, J. H., Hong, Y. S., Oh, S. R., and Suh, I. H., et al., Design of a Parallel-Type Gripper Mechanism, The International Journal of Robotics Research, Vol. 21, No. 7, 2002, pp. 661-76.

[10] Kocabas, H., Gripper Design with Spherical Parallelogram Mechanism, Journal of Mechanical Design, Vol. 131, No. 7, 2009, pp. 075001.

[11] Jiang, L., Guan, Y., Zhou, X., Zhang, X., and Zhang, H., Editors., Grasping Analysis for a Biped Climbing Robot, 2010 IEEE International Conference on Robotics and Biomimetics, 2010, IEEE.

[12] Tavakoli, M., Marques, L., 3DCLIMBER: Climbing and Manipulation Over 3D Structures, Mechatronics, Vol. 21, No. 1, 2011, pp. 48-62.

[13] Mampel, J., Gerlach, K., Schilling, C., and Witte, H., A Modular Robot Climbing On Pipe-Like Structures, 4th International Conference on Autonomous Robots and Agents 2009, Feb 10 ,pp. 87-91, IEEE.

[14] Abderrahim, M., Balaguer, C., Giménez, A., Pastor, J. M., and Padron, V. M., ROMA: A Climbing Robot for Inspection Operations, In Proceedings 1999 IEEE International Conference on Robotics and Automation, 1999, IEEE.

[15] Nagaoka, K., Minote, H., Maruya, K., Shirai, Y., Yoshida, K., Hakamada, T., Sawada, H., and Kubota, T., Passive Spine Gripper for Free-Climbing Robot in Extreme Terrain, IEEE Robotics and Automation Letters, Vol. 3, No. 3, 2018, pp. 1765-70.

[16] Rahman, N., Carbonari, L., Caldwell, D., and Cannella, F., Kinematic Analysis, Prototypation and Control of a Novel Gripper for Dexterous Applications, Journal of Intelligent & Robotic Systems, Vol. 91, No. 2, 2018, pp. 193-206.

[17] Heidari, H., Pouria, M. J., Sharifi, S., and Karami, M., Design and Fabrication of Robotic Gripper for Grasping in Minimizing Contact Force, Advances in Space Research, Vol. 61, No. 5, 2018, pp. 1359-1370.

[18] Bai, G., Kong, X., and Ritchie, J. M., Kinematic Analysis and Dimensional Synthesis of a Meso-Gripper, Journal of Mechanisms and Robotics, Vol. 9, No. 3, 2017, pp. 031017.

[19] Borisov, I. I., Borisov, O. I., Gromov, V. S., Vlasov, S. M., Dobriborsci, D., and Kolyubin, S. A., Design of Versatile Gripper with Robust Control, IFAC-Papers On Line, Vol. 51, No. 22, 2018, pp. 56-61.

[20] Slotine, J. J., Sastry, S. S., Tracking Control of Non-Linear Systems Using Sliding Surfaces, with Application to Robot Manipulators, International Journal of Control, Vol. 38, No. 2, 1983, pp. 465-92.

[21] Slotine, J. J. E., The Robust Control of Robot Manipulators, The International Journal of Robotics Research, Vol. 4, No. 2, 1985, pp. 49-64.

[22] Slotine, J. J. E., Li, W., On the Adaptive Control of Robot Manipulators, the International Journal of Robotics Research, Vol. 6, No. 3, 1987, pp. 49-59.

[23] Huang, A. C., Chen, Y. C., Adaptive Sliding Control for Single-Link Flexible-Joint Robot with Mismatched Uncertainties, IEEE Transactions on Control Systems Technology, Vol. 12, No. 5, 2004, pp. 770-5.

© 2021 IAU, Majlesi Branch

[24] Parra Vega, V., Arimoto, S., Liu, Y. H., Hirzinger, G., and Akella, P., Dynamic Sliding PID Control for Tracking of Robot Manipulators: Theory and Experiments, IEEE Transactions on Robotics and Automation,Vol. 19, No. 6, 2003, pp. 967-76.

[25] Harashima, F., Hashimoto, H., and Maruyama, K., Editors., Practical Robust Control of Robot Arm Using Variable Structure System, Proceedings 1986 IEEE International Conference on Robotics and Automation, 1986, IEEE.

[26] Talole, S., Phadke, S., Model Following Sliding Mode Control Based On Uncertainty and Disturbance Estimator, Journal of Dynamic Systems, Measurement, and Control, Vol. 130, No. 3, 2008, pp. 034501.

[27] Young, K. D., Utkin, V. I., and Ozguner, U., Editors., A Control Engineer's Guide to Sliding Mode Control, Proceedings 1996 IEEE International Workshop on Variable Structure Systems-VSS'96, 1996, IEEE.

[28] Slotine, J. J. E., Li, W., Applied Nonlinear Control: Prentice Hall Englewood Cliffs, NJ, 1991.

[29] Asada, H., Slotine, J. J., Robot Analysis and Control, John Wiley & Sons, 1986.

© 2021 IAU, Majlesi Branch